

# Effect of Geometric Twist on Wind Turbine Blade

S.Sharmila a S.Anand b.

Assistant Professor

M.A.M School Of Engineering, Trichy, India.

Sharmilasharmi047@gmail.com

**Abstract:** Increasing need for fundamental research in rotor aerodynamics and practical aspects, constraints were imposed on the design. An important part of this work is to conduct a study of the design trade-offs to determine the effect of the geometric twist on the wind turbine and its energy capture of the rotor. Another objective was to determine the necessary modifications to the blade geometry and twist in aerofoil for a three-bladed rotor configuration. This project aims to describe the approach and process used to design a tapered/twisted blade, and to provide performance predictions for the conventional wind turbine blade and the updated model with geometric twist. The aerodynamic performance of the blade with and without geometric twist is analysed by using Computational Fluid Dynamics and to increase the lift of the blade and to prevent over speed of the rotor. Additionally, twisted blades tested for its stall delaying characteristics.

**Keywords**—twisted blade, tapered, stall, CFD, oscillation and over pressure.

## I. INTRODUCTION

The Wind it might seem obvious, but an understanding of the wind is fundamental to wind turbine design. The power available from the wind varies as the cube of the wind speed, so twice the wind speed means eight times the power. This is why sites have to be selected carefully: below about 5m/s (10mph) wind speed there is not sufficient power in the wind to be useful. Conversely, strong gusts provide extremely high levels of power, but it is not economically viable to build machines to be able to make the most of the power peaks as their capacity would be wasted most of the time. So the ideal is a site with steady winds and a machine that is able to make the most of the lighter winds whilst surviving the strongest gusts. As well as varying day-to-day, the wind varies every second due to turbulence caused by land features, thermals and weather. It also blows more strongly higher above the ground than closer to it, due to surface friction. All these effects lead to varying loads on the blades of a turbine as they rotate, and mean that the aerodynamic and structural design needs to cope with conditions that are rarely optimal. By extracting power, the turbine itself has an effect on the wind; downwind of the turbine the air moves more slowly than upwind. The wind starts to slow down even before it reaches the blades, reducing the wind speed through the “disc” (the imaginary circle formed by the blade tips, also called the swept area) and hence reducing the available power. Some of the wind that was heading for the disc diverts around the slower-moving air and misses the blades entirely. So there is an optimum amount of power to extract from a given disc diameter: try to take too much and the wind will slow down too much, reducing the available power. In fact the ideal is to

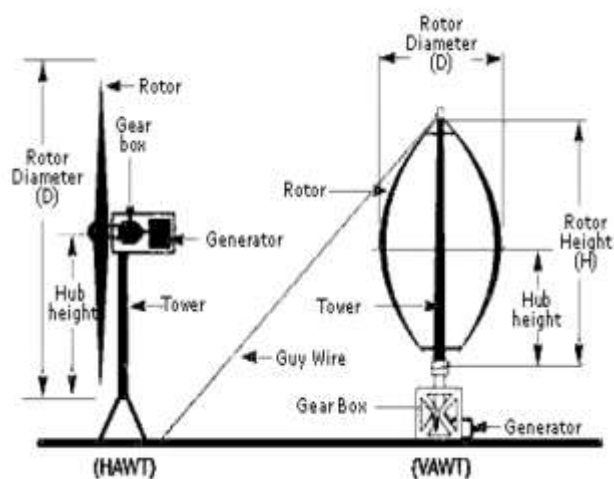
reduce the wind speed by about two thirds downwind of the turbine, though even then the wind just before the turbine will have lost about a third of its speed. This allows a theoretical maximum of 59% of the wind’s power to be captured (this is called Betz’s limit). In practice only 40-50% is achieved by current designs.

## 1.5 WIND TURBINE TYPE

The horizontal wind turbine is a turbine in which the axis of the rotor’s rotation is parallel to the wind stream and the ground. Most HAWTs today are two- or three-bladed, though some may have fewer or more blades. There are two kinds of Horizontal Axis Wind Turbines: the upwind wind turbine and the downwind wind turbine. The HAWT works when the wind passes over both surfaces of the airfoil shaped blade but passes more rapidly at the upper side of the blade, thus, creating a lower-pressure area above the airfoil. The difference in the pressures of the top and bottom surfaces results in an aerodynamic lift. The blades of the wind turbine are constrained to move in a plane with a hub at its center, thus, the lift force causes rotation about the hub. In addition to the lifting force, the drag force which is perpendicular to the lift force impedes rotor rotation.

## 1.8 COMPONENT OF A WIND TURBINE

Wind turbine usually has six main components the rotor, the generator, the gear box, the control and protection system, the tower and the foundation. This main component can be seen in figure.



**1.8.1 Rotor:** the rotor is an elegant aero foil shaped blade which takes the wind and aerodynamically converts its kinetic energy into mechanical energy through a connected shaft.

**1.8.2 Generator:** the generator is a device that produces electricity when mechanical work is given to the system. Control and protection system: the protection system is like a safety feature that makes sure that the turbine will not be working under dangerous condition. This includes a break system triggered by the signal of higher wind speeds to stop the rotor from movement under excessive wind gusts.

**1.8.3 Gear box:** Gear box used in wind energy systems to change low speed high torque power coming from a rotor blade to high speed low torque power which is used for generator. It is connected in between main shaft and generator shaft to increase rotational speeds from about 30 to 60 rotations per minute (rpm) to about 1000 to 1800 rpm. Gearboxes used for wind turbine are made from superior quality aluminum alloys, stainless steel, cast iron etc.

**1.8.4 Nacelle:** A housing which contains all the components which is essential to operate the turbine efficiently is called a nacelle. It is fitted at the top of a tower and includes the gear box, low- and high-speed shafts, generator, controller, and brakes. A wind speed anemometer and a wind vane are mounted on the nacelle.

**1.8.5 Tower:** the tower is the main shaft that connects the rotor to the foundation. It also raises the rotor high in the air where we can find stronger winds. With horizontal axis wind turbines, the tower houses the stair to allow for maintenance and inspection.

**1.8.6 Foundation:** The foundation or the base supports the entire wind turbine and make sure that it is well fixed onto the ground or the roof for small household wind turbine. This is usually consisting of a solid concrete assembly around the tower to maintain its structural integrity.

### III INTRODUCTION TO CFD

CFD provides numerical approximation to the equations that govern fluid motion. Application of the CFD to analyze a fluid problem requires the following steps. First, the mathematical equations describing the fluid flow are written. These are usually a set of partial differential equations. These equations are then discretized to produce a numerical analogue of the equations. The domain is then divided into small grids or elements. All CFD codes contain three main elements: (1) a pre-processor, which is used to input the problem geometry, generate the grid, and define the flow parameter and the boundary conditions to the code. (2) A flow solver, which is used to solve the governing equations of the flow subject to the conditions provided. There are four different methods used as a flow solver: (i) finite difference method; (ii) finite element method, (iii) finite volume method, and (iv) Spectral method. (3)

A post-processor, which is used to massage the data and show the results in graphical and easy to read format.

Due to the nonlinear behavior of the Navier-Stokes equations, solving a whole 3D turbulent flow model of a wind turbine rotor with finest details in a time dependent way is extremely

difficult based on methods such as direct numerical simulation (DNS). Other options like large eddy simulation (LES) and detached eddy simulation (DES) methods are also applied in wind turbine aerodynamics by some researchers. However, to be computationally cost-efficient, RANS equations are most widely used to model the change of flow domain caused by turbulence around wind turbine blades. To obtain a reasonable accurate solution for wind turbine aerodynamics, three key elements are involved:

- (1) A good mesh quality.
- (2) An advanced turbulence model.
- (3) An accurate solve scheme.

### 4.3 GEOMETRY AND MESH

To model a wind turbine rotor using the CFD method, an exact 3D geometry of the wind turbine rotor is needed in a digitized format, usually in a "computer aided design" (CAD) format. A small wind turbine blade is generally twisted and tapered. The sectional airfoil of the blade is a shape often with a small rounded leading edge, and a sharp trailing edge or thin blunt trailing edge. A sufficient resolution of the boundary layer mesh is needed to solve the boundary layer around the blade surfaces. To secure an accurate solution in the boundary flow, the dimensionless cell wall distance  $Y^+$  should be below or at least approximated to 1. Additionally, a large-enough flow domain is needed to avoid disturbances from the domain boundary surfaces, and a fine enough time step is preferable to generate a good result. However, a good match between mesh refinement, mesh quality, domain size and time step refinement is very important to produce a quality result, i.e. accurate solution and reasonable computation cost.

### 4.4 TURBULENCE AND TRANSITION

To explore the flow field near rotating wind turbine blades, there are several turbulence models presented with good results for wind turbine airfoil and rotor aerodynamics analysis: Spalart-Allmaras (S-A) model, standard k-epsilon ( $k-\epsilon$ ) model, k-omega ( $k-\omega$ ) model, Shear Stress Transport (SST)  $k-\omega$  model, and transition SST model. The details of these models can be found. In Villalpando's research, it was reported that, the SST  $k-\omega$  model has a better agreement with experimental results than other turbulence models such as the S-A model, the  $k-\epsilon$  model and the Reynolds Stress Model (RSM).

However, when stall occurs, the conclusion was drawn that the transition location is crucial for the simulation and the Menter's SST transition model was claimed to have better agreement with experiment results than other models. In the transition SST model, the transition equations (i.e. one is for the intermittency  $\gamma$  and the other is for the transition momentum thickness Reynolds number  $Re\theta^*$ ) interact with the SST  $k-\omega$  turbulence model. Due to two additional transport equations involved, it is apparent that the transition model is more time-consuming and more sensitive to converge than the SST  $k-\omega$  model. Some research works aimed to find a middle way. Catalano performed a RANS analysis using the SST  $k-\omega$

model with an imposed transition location which is 10% offset downstream from the predicted point of a fully turbulence model. However, the offset is based on experience in this approach. Instead of using imposed variables to catch the transition phenomenon like turbulence models and without imposing transition location, the transition SST model was reported to have a promising accuracy in predicting transition flows. Many research works have been done regarding to the transition model. The Menter's transition model was investigated on the 2D S809 airfoil and better agreements have been achieved for angle of attack from  $0^\circ$  to  $9^\circ$ , and it was indicated that the difference at high angle of attacks was more possibly caused by the 3D flow effects which 2D simulation model cannot capture. A full 3D wind turbine rotor which uses the S809 airfoil were accomplished in Langtry's research, the transition model was reported to be compatible with modern CFD techniques such as unstructured grids and massively parallel execution, and the transition model was claimed to be well suited to predict wind turbine rotor aerodynamics.

#### IV DERIVATION OF RANS EQUATION

Applying the fundamental laws of mechanics to a fluid gives the governing equations for a fluid. The conservation of mass equation is

$$\frac{\partial \rho}{\partial t} + \nabla \cdot (\rho \vec{V}) = 0$$

Momentum equation,

$$\rho \frac{\partial \vec{V}}{\partial t} + \rho (\vec{V} \cdot \nabla) \vec{V} = -\nabla p + \rho \vec{g} + \nabla \cdot \tau_{ij}$$

The equations governing the fluid motion are the three fundamental principles of mass, momentum, and energy conservation.

$$\text{Continuity} \quad \frac{\partial \rho}{\partial t} + \nabla \cdot (\rho \vec{V}) = 0$$

$$\text{Momentum} \quad \rho \frac{D\vec{V}}{Dt} = \nabla \cdot \tau_{ij} - \nabla p + \rho \vec{F}$$

$$\text{Energy} \quad \rho \frac{De}{Dt} + p(\nabla \cdot \vec{V}) = \frac{\partial Q}{\partial t} - \nabla \cdot \mathbf{q} + \Phi$$

##### 4.7.1 Elliptic:

Laplace equation is a familiar example of an elliptic type equation.

$$\nabla^2 u = 0$$

Where  $u$  is the fluid velocity. The incompressible irrotational flow (potential flow) of a fluid is represented by this type of equation. Another practical example of this equation is the steady state pure heat conduction in a solid, i.e.,  $\nabla^2 T = 0$ , as can be readily obtained from equation.

##### 4.7.2 Hyperbolic:

Qualitative properties of hyperbolic equations can be explained by a wave equation.

$$\frac{\partial^2 u}{\partial t^2} = c^2 \frac{\partial^2 u}{\partial x^2}$$

Where  $c$  is the wave speed. In this case, values of solution depend locally on the initial conditions. The propagation signal speed is finite. Continuous boundary and initial values can give rise to discontinuity. Solution is no more continuous and therefore shocks can be observed and captured in this class of equations. Depending on the flow, the governing equations of fluid motion can exhibit all three classifications.

#### 4.8 BOUNDARY CONDITIONS:

The governing equation of fluid motion may result in a solution when the boundary conditions and the initial conditions are specified. The form of the boundary conditions that is required by any partial differential equation depends on the equation itself and the way that it has been discretized. Common boundary conditions are classified either in terms of the numerical values that have to be set or in terms of the physical type of the boundary condition.

For steady state problems there are three types of spatial boundary conditions that can be specified

Dirichlet boundary condition

$$\phi = f_1(x, y, z)$$

$$\frac{\partial \phi}{\partial n} = f_2(x, y, z)$$

Neuman boundary condition:

Mixed type boundary condition:

The physical boundary conditions that are commonly observed in the fluid problems are as follows

$$a\phi + b \frac{\partial \phi}{\partial n} = f_3(x, y, z)$$

**4.8.1 Solid walls:** Many boundaries within a fluid flow domain will be solid walls, and these can be either stationary or moving walls. If the flow is laminar then the velocity components can be set to be the velocity of the wall. When the flow is turbulent, however, the situation is more complex.

**4.8.2 Inlets:** At an inlet, fluid enters the domain and, therefore, its fluid velocity or pressure, or the mass flow rate may be known. Also, the fluid may have certain characteristics, such as the turbulence characterizes which needs to be specified.

**4.8.3 Symmetry boundaries:** When the flow is symmetrical about some plane there is no flow through the boundary and the derivatives of the variables normal to the boundary are zero.

**4.8.4 Cyclic or periodic boundaries:** These boundaries come in pairs and are used to specify that the flow has the same

values of the variables at equivalent positions on both of the boundaries.

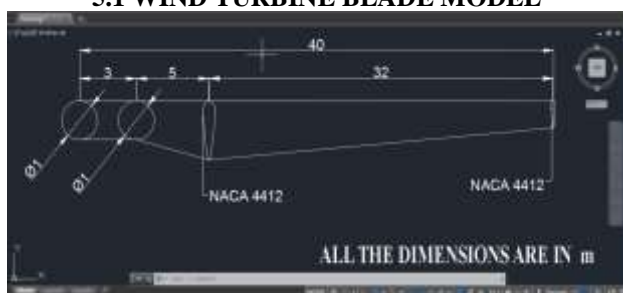
#### 4.11 UNSTRUCTURED GRID

Unstructured grids have the advantage of generality in that they can be made to conform to nearly any desired geometry. This generality, however, comes with a price. The grid generation process is not completely automatic and may require considerable user interaction to produce grids with acceptable degrees of local resolution while at the same time having a minimum of element distortion. Unstructured grids require more information to be stored and recovered than structured grids (e.g., the neighbor connectivity list), and changing element types and sizes can increase numerical approximation errors.

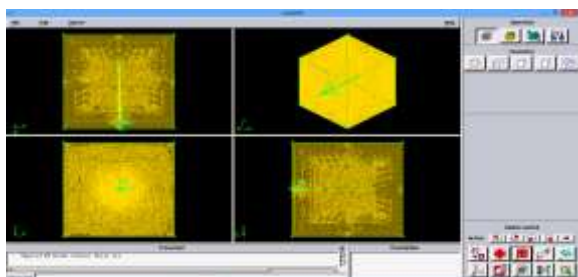
A popular type of unstructured grid consists of tetrahedral elements (Fig. 15). These grids tend to be easier to generate than those composed of hexahedral.

### V WIND TURBINE BLADE MODEL

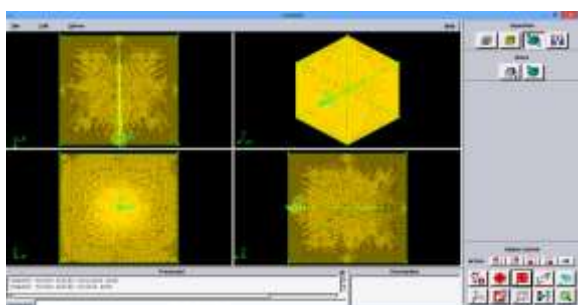
#### 5.1 WIND TURBINE BLADE MODEL



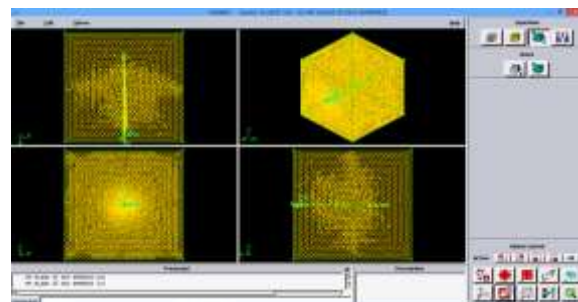
#### 5.2 TAPERED WIND TURBINE BLADE WITHOUT TWIST .



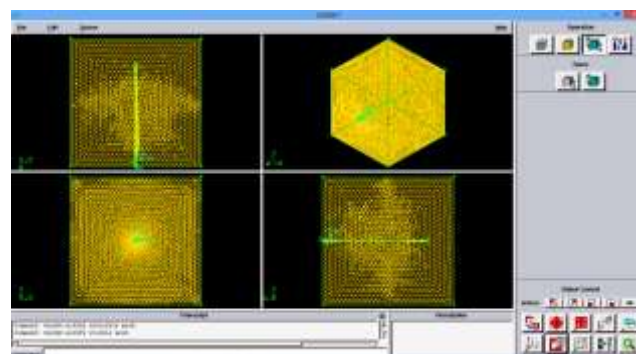
#### 5.3 WIND TURBINE BLADE WITH TWIST IN 25 DEGREE WASH IN



#### 5.4 WIND TURBINE BLADE WITH TWIST IN 45 DEGREE WASH IN



#### 5.5 WIND TURBINE BLADE WITH TWIST IN 25 DEGREE WASHOUT



### VI ANALYSIS OF WIND TURBINE BLADE MODEL

#### 6.1 TAPERED BLADE WITHOUT TWIST

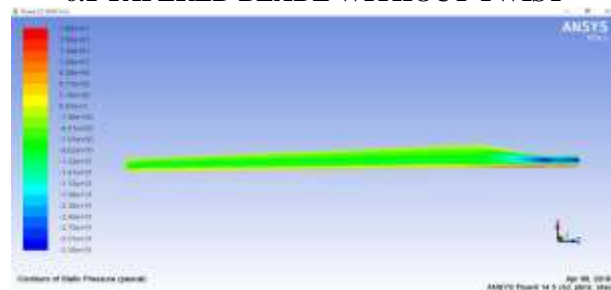


Figure 6.1: static pressure top view



Figure 6.2: static pressure bottom view

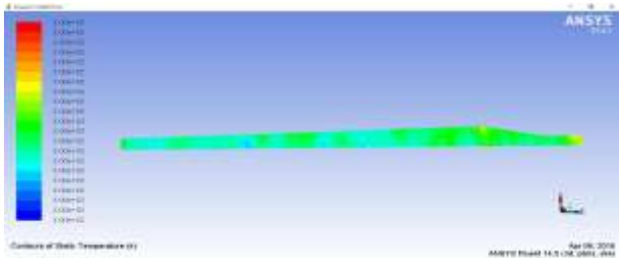


Figure 6.3: static temperature top view

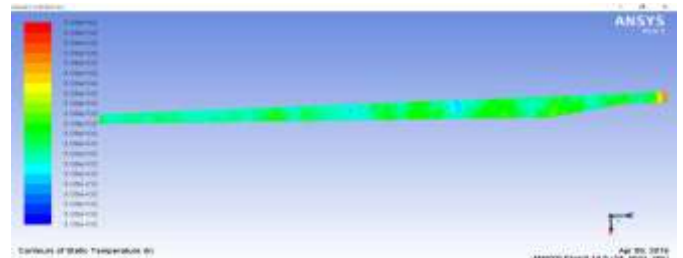


Figure 6.8: static temperature bottom view`

6.3 TAPERED BLADE WITH TWIST 45 DEGREE WASH IN

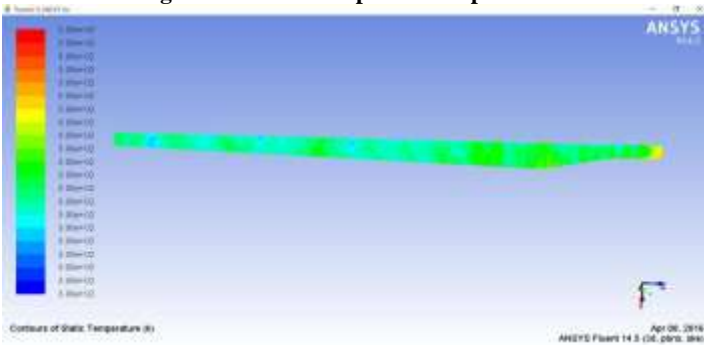


Figure 6.4: static temperature bottom view

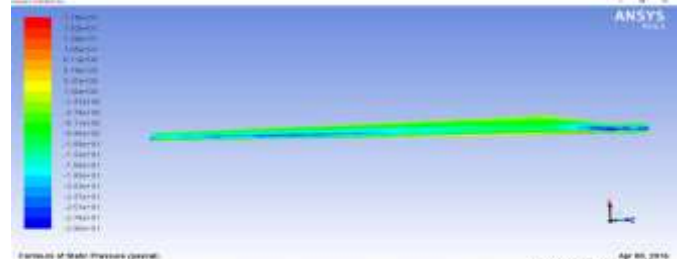


Figure 6.9: static pressure top view

6.2 TAPERED BLADE WITH TWIST 25 DEGREE WASH IN

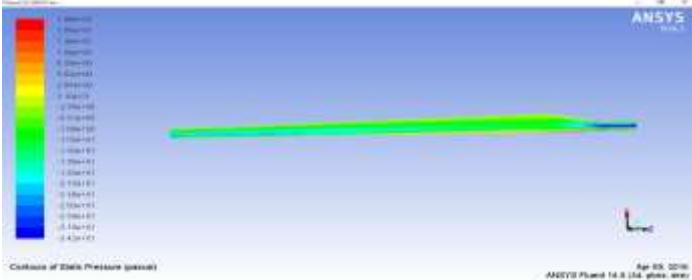


Figure 6.5: static pressure top view

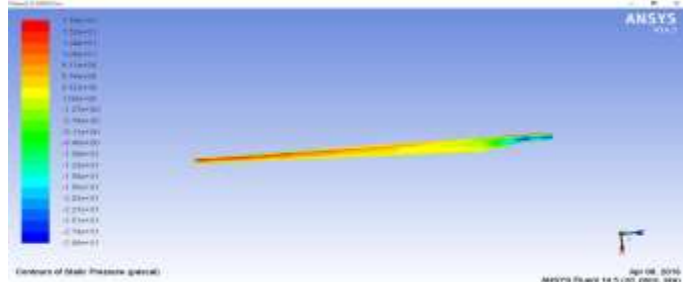


Figure 6.10: static pressure bottom view

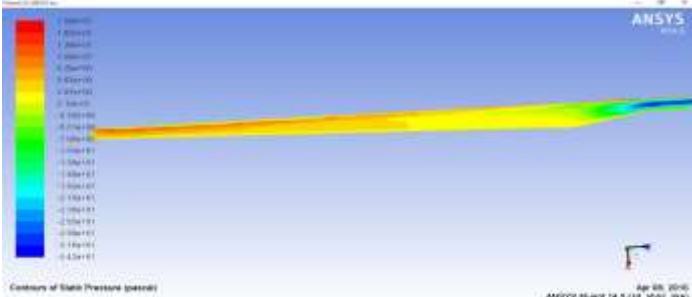


Figure 6.6: static pressure bottom view

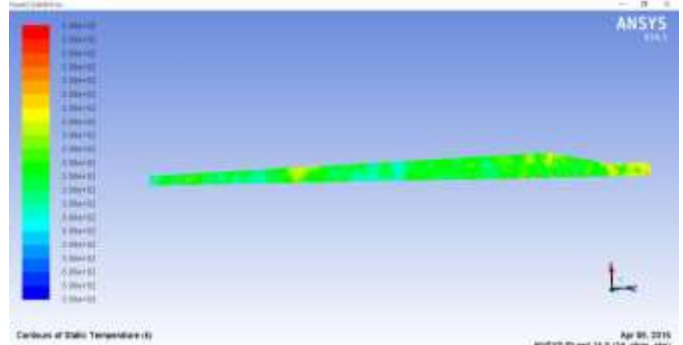


Figure 6.11: static temperature top view

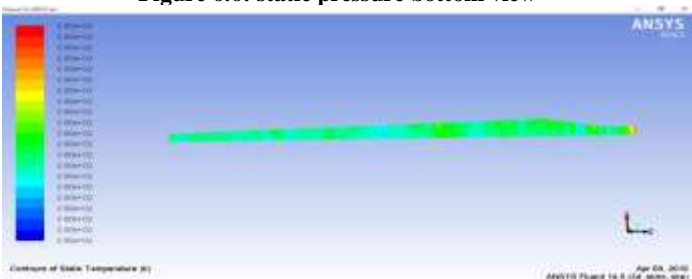


Figure 6.7: static temperature top view

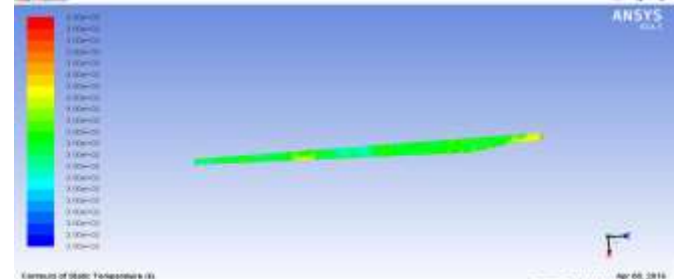


Figure 6.12: static temperature bottom view



**6.4 TAPERED BLADE WITH TWIST 25 DEGREE WASH OUT**

**6.5 TAPERED BLADE WITH TWIST 45 DEGREE WASH OUT**

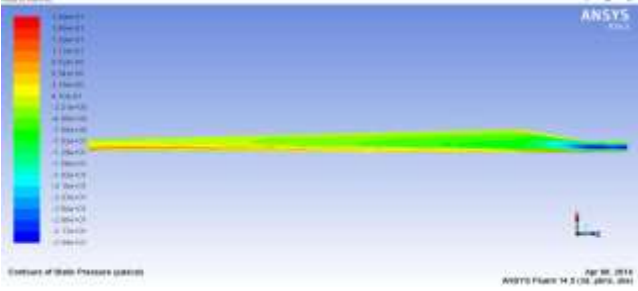


Figure 6.13: static pressure top view

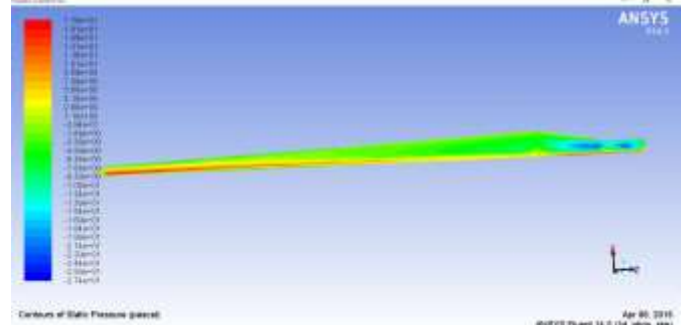


Figure 6.17: static pressure top view

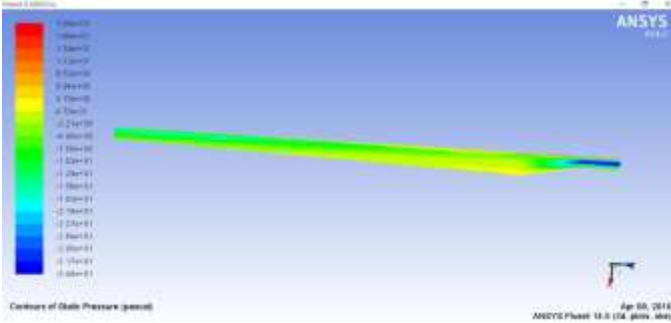


Figure 6.14: static pressure bottom view

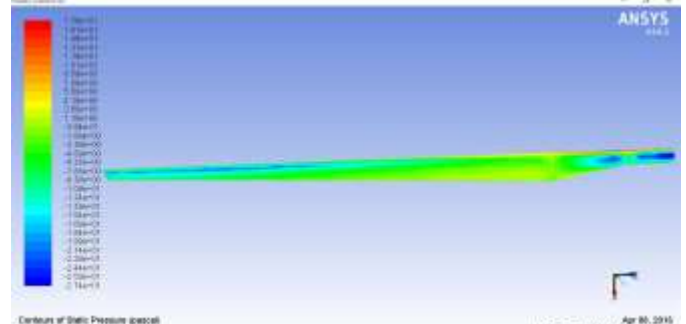


Figure 6.18: static pressure bottom view

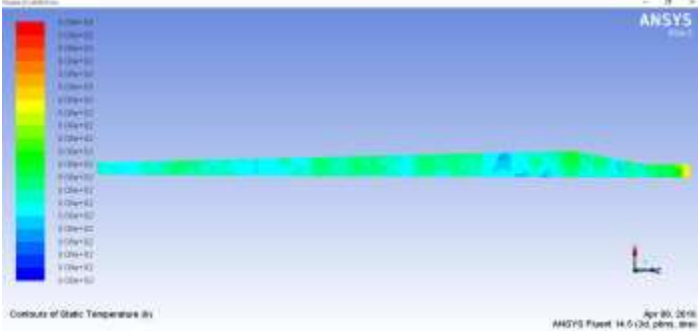


Figure 6.15: static temperature top view

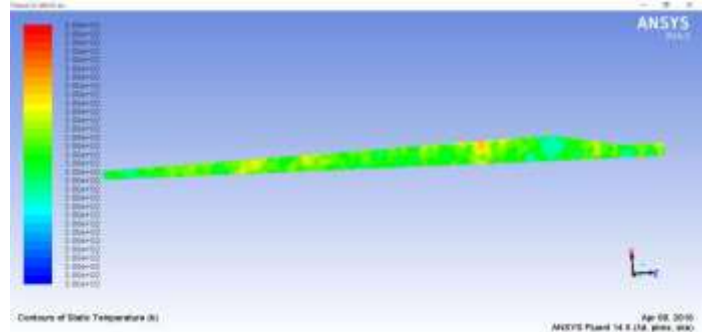


Figure 6.19: static temperature top view

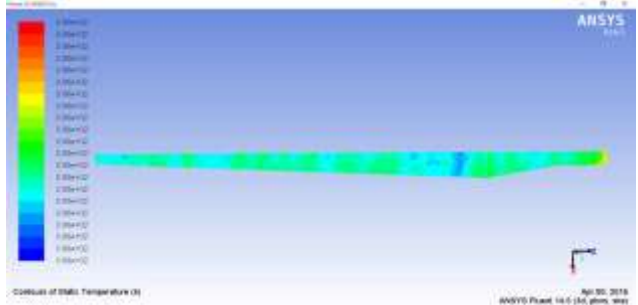


Figure 6.16: static temperature bottom view

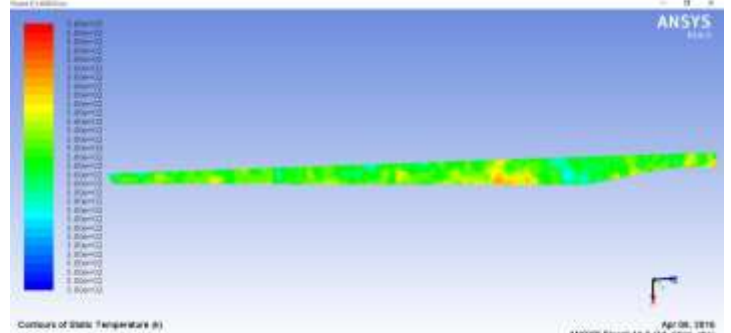


Figure 6.20: static temperature bottom view

## VII RESULTS AND DISCUSSION

### 7.1 DETERMINATION OF LIFT TO DRAG RATIO

Table 7.1: Determination Lift to Drag Ratio L/D

BLADE TYPE	LIFT	DRAG	LIFT/DRAG RATIO
CONVENTIONAL TAPERED BLADE	14.02	7.10	1.97
25° DOWN	-14.6	12.78	-1.14
25° UPWARD	49.54	13.38	3.70
45° DOWN	-28.02	23.57	-1.19
45° UPWARD	56.89	23.18	2.45

## VIII CONCLUSION

The lift to drag ratio of the wind turbine blade with and without geometric twist is analysed by using Computational Fluid Dynamics. We are selected the twist angles 25, 45 in wash out and wash in condition to analyse the lift to drag ratio. In this analysis 25 degree wash in condition is gives the result of 46 % higher than conventional blade and to increase the lift of the blade and prevented the over speed of the rotor. Finally the increase the stall delay of the rotor.

## REFERENCES

- 1) Hardikpatel, Sanatdamania "Performance Prediction of Horizontal Axis Wind Turbine Blade" - May 2013.
- 2) Farooq Ahmad Najar, G A Harmain "Blade Design and Performance Analysis of Wind Turbine" - June 2013.
- 3) G.Sivaraj, Mr. M Gokul raj "Optimum Aerodynamic Design in Wind Mill Blades using Winglet function" Prof, - May 2012.
- 4) L.Wanga, X. Tanga, X. Liub "Optimized chord and twist angle distributions of wind turbine blade considering Reynolds number effects" - 2012.
- 5) Mohammad Shamsavarifard, Eric Louis Bibeau n,"Effect of shroud on the performance of horizontal axis hydrokinetic turbines" - 21 January 2015.
- 6) H. V. Mahawadiwar, V.D. Dhopte, P.S.Thakare, Dr. R. D. Askhedkar"Cfd Analysis of Wind Turbine Blade"Vol-2, Issue-3, pp-3188-3194, 2012
- 7) R.S. Amano, R.J. Malloy "CFD Analysis on Aerodynamic Design Optimization of Wind Turbine Rotor Blade", pp 71-75 2009
- 8) kentaro hayashi, hiroshi nishino, hiroyuki hosoya, koji fukami, tooru matsuo, takao kuroiwa "Low- noise Design for Wind Turbine Blades", Vol-49, pp-74-772012
- 9) Horia dumitrescu, Vladimir Cardos Florin Frunzulica, Alexandru DUMITRACHE "Determination of angle of attack for rotating blades"Volume-4, Issue-2, 2012
- 10) s. rajakumar, dr.d.ravindran "computational fluid dynamics of wind turbine blade at various angles of attack and low reynolds number", vol-2(11), 2010 55